Pflügers Arch – Eur J Physiol (1998) 435:375–381

ORIGINAL ARTICLE

**Xinjun He · Gemma A. J. Kuijpers · Gertrud Goping
Jill A. Kulakusky · Changyu Zheng · Christine Delporte
Chung-Ming Tse · Robert S. Redman · Mark Donowitz
Harvey B. Pollard · Bruce J. Baum**

A polarized salivary cell monolayer useful for studying transepithelial fluid movement in vitro

Received: 16 September 1997 / Accepted: 17 September 1997

Abstract There are no reported, convenient in vitro models for studying polarized functions in salivary epithelial cells. Accordingly, we examined three often-used salivary cell lines for their ability to form a polarized monolayer on permeable, collagen-coated polycarbonate filters. Only the SMIE line, derived from rat submandibular gland, had this ability. The SMIE cell monolayer exhibited junctional complexes, with a tight-junction-associated protein, ZO-1, localized to cell–cell contact areas. The Na^+/K^+-ATPase α_1-subunit was detected predominantly in the basolateral membranes, while the Na^+/H^+ exchanger isoform 2 appeared primarily in the apical membranes. Using adenovirus-mediated cDNA transfer, SMIE cells were shown to be capable of routing marker proteins (β-galactosidase ± a nuclear targeting signal, α1-antitrypsin, aquaporin-1) to appropriate locations. Furthermore, this salivary cell monolayer provided a convenient tool for studying aquaporin-1-mediated, osmotically directed, transepithelial fluid movement in vitro. Thus, SMIE cells appear to be a useful experimental model with which to study some polarized functions in a salivary epithelial cell line.

X. He · J.A. Kulakusky · C. Zheng · C. Delporte · B.J. Baum (✉)
Gene Therapy and Therapeutics Branch,
National Institute of Dental Research, 10 Center Drive,
MSC 1190, Bldg 10/Rm 1N113, Bethesda MD 20892-1190, USA

G.A.J. Kuijpers · G. Goping · H.B. Pollard
Department of Anatomy and Cell Biology,
Uniformed Services University of the Heath Sciences,
Bethesda MD 20814, USA

C.-M. Tse · M. Donowitz
Departments of Physiology and Medicine,
Division of Gastroenterology,
The Johns Hopkins University School of Medicine,
Baltimore MD 21205, USA

R.S. Redman
Oral Pathology Research Laboratory,
Department of Veterans Affairs Medical Center,
Washington DC 20422, USA

Key words Salivary gland · Epithelial cell · Polarity · Protein targeting · Aquaporin-1 · Facilitated fluid movement

Introduction

Salivary glands have long been used as models for studying exocrine physiology due to their convenient anatomical position, and the fact that their epithelial cells carry out specialized vectorial transport functions. The acinar cells (and possibly the intercalated duct cells) are considered relatively water permeable and secrete an isotonic plasma-like primary fluid, whereas most duct cells are considered relatively water impermeable and resorb Na^+ and Cl^- ions, resulting in a hypotonic final saliva being secreted into the mouth [2, 5, 27]. As with other epithelia, the formation and maintenance of the salt gradients is a result of the polarized organization of cells into specific apical and basolateral plasma membrane domains. The two domains are morphologically and biochemically distinct, separated by tight junctions, and are composed of different proteins and lipids [22].

The mechanisms underlying the polarized distribution of plasma membrane proteins to the apical and the basolateral domains are, thus, of fundamental importance for understanding the secretory and absorptive functions of salivary glands. General studies of the mechanisms responsible for epithelial cell polarity have been aided greatly by the availability of epithelial cell lines which, when grown in vitro on permeable substrata, retain key aspects of the morphological and functional polarity associated with naturally occurring epithelia [4]. Indeed, a number of epithelial cell lines have been extensively characterized in this regard, including MDCK from dog kidney [4], LLC-PK1 from pig kidney [23], A6 from toad bladder [20], Caco-2 from a human colonic tumor [10] and T84 from a human colonic carcinoma [9]. There are no reports of such information on cells derived from salivary glands. Herein, we describe an in vitro model system useful for studying polarized functions in a salivary epithelial cell line.

Materials and methods

Cell cultures

The SMIE cell line is derived from rat submandibular gland epithelial cells immortalized with the adenovirus 12S E1A gene product [12]. A5 cells are a clonal line derived from rat submandibular ducts [11]. HSG cells are derived from an irradiated human submandibular gland and were a generous gift of Dr. Mitsunabo Sato (Tokushima University, Japan) [24]. SMIE and A5 cells were maintained on 100-mm-diameter plastic Petri dishes (GibcoBRL, Gaithersburg, Md., USA) in a humidified incubator at 37°C under a 5% CO_2 atmosphere in Dulbecco's modified Eagle's medium (DMEM), with a low glucose concentration (1.0 g/l) (Biofluids, Rockville, Md., USA), supplemented with 10% heat-inactivated fetal bovine serum (HyClone, Logan, Utah, USA), 100 units/ml penicillin, 100 μg/ml streptomycin, and 2 mM L-glutamine (Biofluids). HSG cells were grown in a 1:1 mixture of DMEM and Ham's F-12 medium with the above supplements. Cells were subcultured by trypsinization once a week and fed every 2 or 3 days. For experiments, approximately 3×10^6 cells were plated on 24.5-mm-diameter (4.71 cm^2), 0.45-μm pore size, types I and III collagen-coated, Transwell-Col polycarbonate filter inserts (Costar, Cambridge, Mass., USA). The upper and lower chambers contained 1.5 and 2.6 ml growth media, respectively.

Light and transmission electron microscopy

Cells grown on a polycarbonate filter were fixed in 2% glutaraldehyde in 0.1 N cacodylate buffer (pH 7.4) containing 2% sucrose for 1 h at room temperature. Filters with fixed cells were cut into small pieces. Samples were washed in buffer for 3×10 min on ice, and postfixed in 1% OsO_4 containing 1% sucrose and 1% potassium ferricyanide for 1 h on ice. In order to accurately identify the nature of the components of the junctional complexes between cells [3], the following preparatory steps were employed (Dr. M. Brightman, NINDS, NIH, Bethesda, Md.,USA, personal communication). Samples were washed for 3×5 min in cold 0.1 N sodium acetate buffer (pH 5.0) at 4°C. Subsequently, en bloc staining of samples was carried out with cold 1% uranyl acetate in 0.1 N sodium acetate buffer overnight at 4°C. Samples were then washed 3×5 min in cold sodium acetate buffer at 4°C. Finally, samples were washed once more in 0.1 N cacodylate buffer, dehydrated through a graded series of ethanol solutions, and embedded in Epon or Unicryl. Polymerization of Unicryl was carried out by UV light at –50°C.

Semithin (0.8–1 μm) sections were cut perpendicular to the substratum on a Reichert Ultracut FC4 ultramicrotome. Sections were stained with toluidine blue for 3–6 min, washed with H_2O, air-dried, and embedded in Cytoseal 60 (Stephen Scientific, Riverdale, N.J., USA) for examination with a Zeiss Axiophot light microscope. Ultrathin sections (70–80 nm) were collected on 400-mesh hexagonal Cu grids, stained with uranyl acetate and lead citrate in an LKB Ultrostainer (Bromma, Sweden), and examined using a Philips TEM 400 electron microscope at an accelerating voltage of 80 kV.

Laser scanning confocal microscopy

Cells grown on filters were subjected to immunofluorescence staining for either the α_1-subunit of the Na^+/K^+-ATPase, the Na^+/H^+ exchanger isoform 2 (NHE2) or a tight-junction-associated protein (ZO-1) according to the method described by Marrs et al. [17] with minor modifications. Briefly, cells were rinsed with PBS (phosphate-buffered saline, pH 7.4, Biofluids) and fixed with prechilled (–70°C) 100% methanol on dry-ice for 15 min. Fixed cells were rinsed with PBS and blocked with 5% donkey serum (Jackson ImmunoResearch, West Grove, Pa.,USA) in PBS containing 0.2% bovine serum albumin (BSA, Calbiochem, La Jolla, Calif., USA) for 20 min. Cells were incubated for 1 h with primary antibodies – either a monoclonal antibody against the α_1-subunit of the Na^+/K^+-ATPase (a gift of Dr. Michael Caplan, Yale University), a polyclonal antibody against NHE2 [26] or a monoclonal antibody against ZO-1 (Chemicon, Temecula, Calif., USA), a 225-kDa protein that is localized exclusively to the cytoplasmic surface of the tight junctions in a variety of epithelia [25]. Primary antibodies were diluted 1:250 in PBS containing 0.2% BSA. Cells were then washed for 3×5 min in PBS containing 0.2% BSA, and incubated for 20 min with the secondary antibodies, fluorescein-isothiocyanate-(FITC-) conjugated donkey anti-mouse or anti-rabbit immunoglobulin G (IgG, Jackson ImmunoResearch) diluted 1:150 in PBS containing 0.2% BSA. Cells were then washed twice in PBS containing 0.2% BSA, and twice in PBS alone. Pieces of filter with cells attached were excised and mounted on Silanated glass slides (Digene, Beltsville, Md., USA) in Citifluor glycerol/PBS mixture (Ted Pella, Redding, Calif., USA). Slides were examined using a Nikon Optiphot II photomicroscope (Melville, N.Y., USA) equipped with an MRC-1000 laser scanning confocal imaging system (Bio-Rad Life Science, Hercules, Calif., USA), using a Krypton/Argon laser as the light source, as recently described [6, 14].

Adenovirus-mediated cDNA transfer and assessment of foreign protein routing

Cells grown on filters were infected with a multiplicity of infection ≈80 of either Ad.RSVβgal (a recombinant adenovirus encoding β-galactosidase with a nuclear localization signal; [1]), Ad-CMVβgal (a recombinant adenovirus encoding β-galactosidase without a targeting signal; [1]), AdhAQP1 (a recombinant adenovirus encoding human aquaporin-1, an integral plasma membrane protein; [7]), and Adα1AT (a recombinant adenovirus encoding human α1-antitrypsin; [1]). One day following infection, cell cultures were examined for the location of these proteins. β-Galactosidase activity was detected histochemically using X-Gal (Boehringer Mannheim, Ind., IN, USA) as a chromogenic substrate [18]. Aquaporin-1 was detected by confocal microscopy, as above, using an affinity-purified antibody [16]. α1-Antitrypsin in culture media and cell lysates was measured with an enzyme-linked immunosorbent assay (ELISA) assay as described [18].

Measurement of net fluid movement across SMIE cell monolayers

Net fluid movement across SMIE cell monolayers in response to an osmotic gradient was determined essentially as described previously [6, 7]. This method represents a modification of a technique described originally by Neufeld et al. [19]. Briefly, SMIE cells were grown to confluence on collagen-coated filter inserts as described above, and then infected with AdhAQP1 [7] or AdCMV-hGH, a genetically identical virus but which encodes human growth hormone (He et al. manuscript submitted for publication), at a multiplicity of infection of ≈5. After 24 h, the medium in the apical chamber was removed and a hyperosmotic medium (440 mosmol/l, i.e. 100 mM sucrose in culture medium) added. The medium in the basal chamber was replaced with fresh isosmotic medium (340 mosmol/l; DMEM-low glucose, above). Transepithelial fluid movement was measured after 60 min.

Results

Monolayer formation of SMIE cells grown on permeable filters

Light microscopy examination of filters between 1 and 7 days of culture showed that SMIE cells formed a continuous monolayer of uniform cells 1 day after plating on the collagen-coated polycarbonate filters (Fig. 1A). Seven days after plating the monolayer grew more compact, with narrower but taller cells (Fig. 1B). These cells displayed the polygonal-shaped, cobblestone appearance

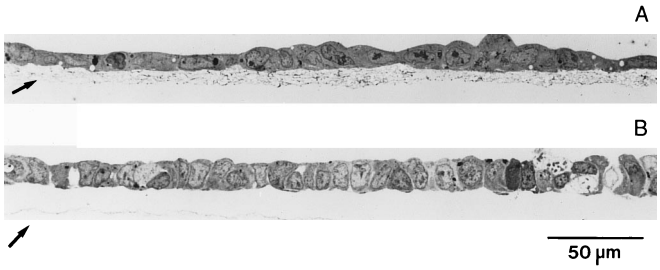

Fig. 1A, B SMIE cell monolayer grown in low-glucose medium as seen by light microscopy. The cells form a continuous monolayer. **A** One day after plating. **B** Seven days after plating. *Arrows* point to the collagen-coated polycarbonate filters. *Bar* = 50 µm

that is characteristic of cultured epithelial cells. Electron microscopy examination (Fig. 2) revealed that the apical surfaces contain short microvilli whereas the lateral surfaces are characterized by numerous interdigitations. Nuclei were generally located basally, often beneath the well-developed Golgi complex. Scattered profiles of rough endoplasmic reticulum were present around the nucleus and in the apical part of the cytosol. Mitochondria were often observed adjacent to the cisternae of the rough endoplasmic reticulum. Numerous free ribosomes occurred throughout the cytoplasm. A single cilium was occasionally observed on the apical surface of a cell (not shown). When samples were prepared by block staining with uranyl acetate [3], and embedded in the acrylic resin Unicryl, there was unequivocal evidence that tight junctions with a pentalaminar appearance were present between adjacent SMIE cells (Fig. 2). When cell monolayers were examined in the *xy* plane using an antibody to detect ZO-1, a tight-junction-associated protein, immunofluorescence staining showed a characteristic [25] perijunctional ring (Fig. 3). Using vertical optical sectioning (*xz* plane), ZO-1 could be localized to sites of cell–cell contact in the apical–lateral region (Fig. 3). Immediately subjacent to the apical membrane, a meshwork of fine filaments connected to the tight junctions (Fig. 2). This was interpreted as a terminal web. Desmosomes were also observed in cells, as soon as 1 day after plating, but were generally rudimentary and relatively uncommon (not shown). In Epon-embedded cells, tight junctional ultrastructure was much less clearly defined (not shown). In contrast to SMIE cells, A5 cells grew in unpolarized, multiple layers and exhibited frequent "holes" (not shown). HSG cells were unable to form an intact monolayer on the filters used here.

Polarized distribution of membrane proteins

We next examined the SMIE cell monolayers to determine if they were able to maintain the ability to sort the Na^+/K^+-ATPase correctly. This essential endogenous plasma membrane protein is targeted to the basolateral membrane domain of rat submandibular epithelial cells in vivo [14]. The α_1-subunit of the Na^+/K^+-ATPase was detected solely on the cell surface of SMIE cells (Fig. 4A). Specifically it was localized by *xz* vertical section to the basolateral cell surface (Fig. 4B). By contrast, a non-selective, general immunostaining of A5 cells was evident throughout the plasma membrane (not shown).

We also examined SMIE cells for evidence of NHE2 [26]. Western blots of plasma membrane preparations from SMIE cell cultures demonstrated the specific expression of NHE2 by these cells, while immunofluores-

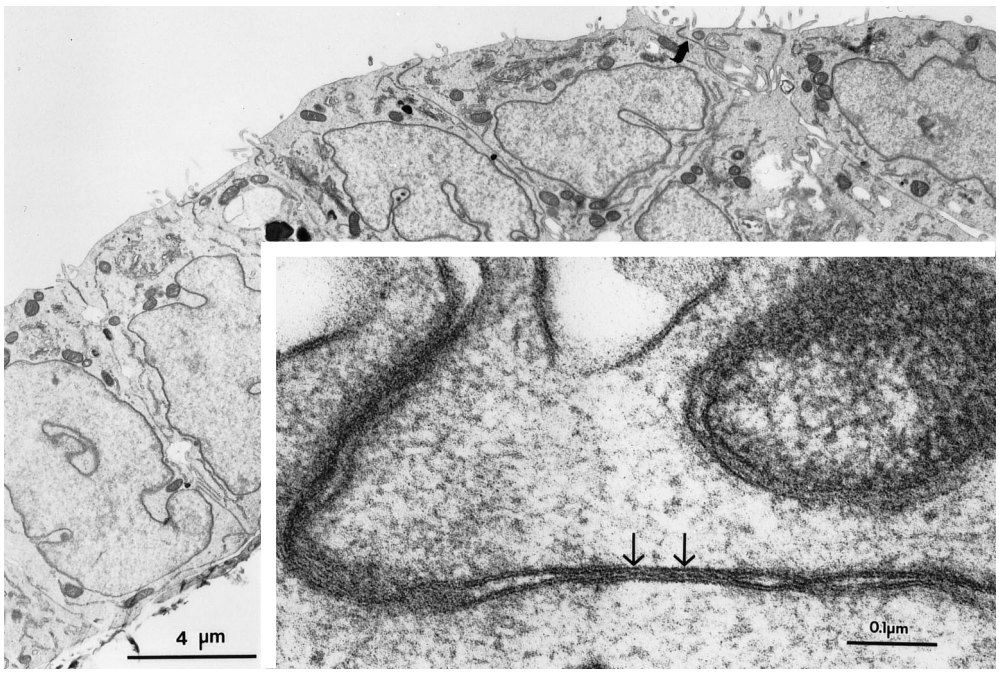

Fig. 2 Electron micrograph of SMIE cells. Cells were cultured for 4 days, and formed a continuous monolayer. Intracellular compartments that can be clearly distinguished are nuclei, mitochondria, lysosomes, the Golgi system and endoplasmic reticulum. Junctional complexes between cells are present at the apical side of the cell layer (*thick arrow at top*). *Bar* = 4 µm. *Inset*: magnification of a junctional complex between two SMIE cells, indicated by the *thick arrow*. Within this junctional area distinct foci are present (*two thin arrows*) where the cell membranes are so closely apposed that they form tight junctions with a typical pentalaminar appearance ("zonulae occludentes"). *Bar* = 0.1 µm

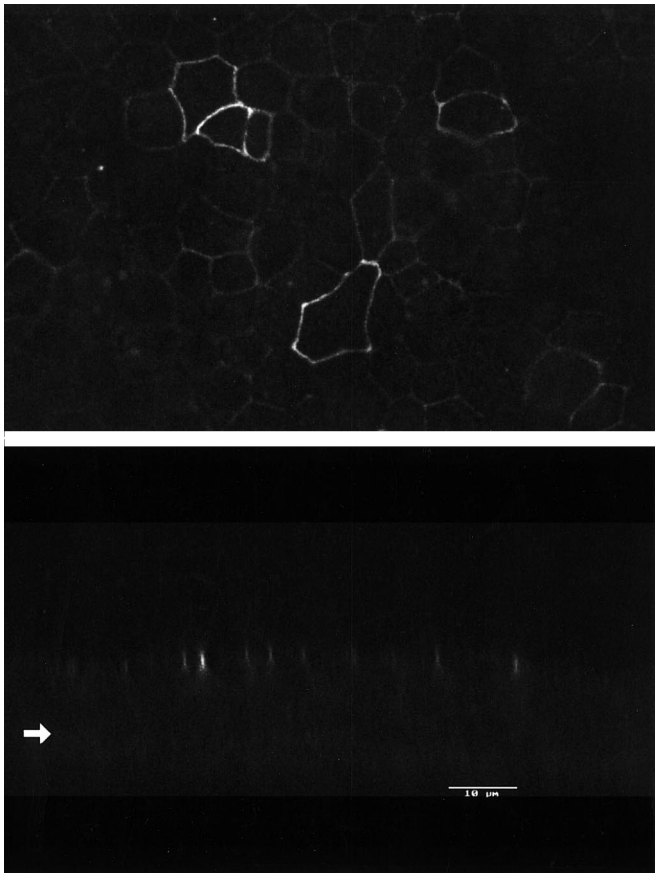

Fig. 3 Immunolocalization of (ZO-1) in SMIE cells. SMIE cells were grown on collagen-coated filters for 4 days, fixed and processed for immunofluoescence using a monoclonal antibody against ZO-1 as described in Materials and methods. The *upper-panel image* is a confocal micrograph of a horizontal (*xy*) optical section through the SMIE cell monolayer at a level toward the apical surface. The *lower-panel image* is a confocal micrograph of a vertical (*xz*) optical section of the cell monolayer at a *z*-step of 0.2 μm. The *arrow* is at the *top* of the collagen-coated polycarbonate filter

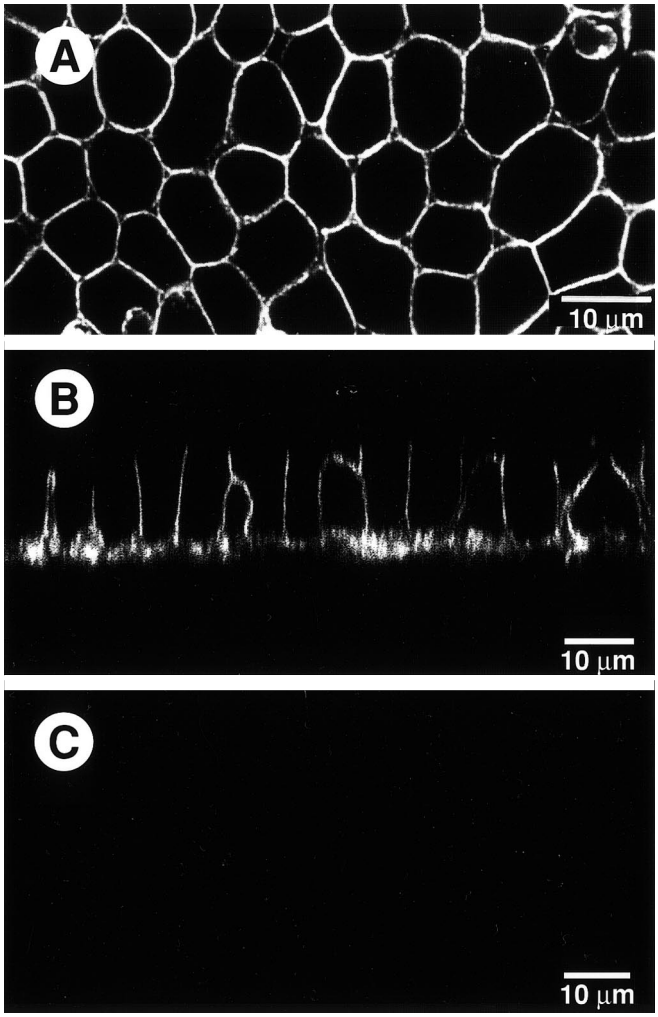

Fig. 4A–C Immunolocalization of the Na^+/K^+-ATPase in SMIE cells. SMIE cells, grown on collagen-coated polycarbonate filters, were fixed and processed for immunofluorescence using a monoclonal antibody against the α_1-subunit of the Na^+/K^+-ATPase as described in Materials and methods. **A** A confocal micrograph of a horizontal (*xy*) optical section through a SMIE cell monolayer of a 4-day-old culture at the level of the cell nuclei. **B** A confocal micrograph of a vertical (*xz*) optical section of a SMIE cell monolayer cultured for 7 days. The negative control (**C**) shown is a 4-day-old cell monolayer incubated with the secondary antibody only

cence staining of SMIE cell monolayers resulted in a focal, lace-like, regular pattern of NHE2 limited to the apical portion of the cells (not shown). When these experiments were repeated using an antibody preincubated with an NHE2 fusion protein [26], Western blot and positive immunofluorescence results were eliminated (not shown).

Assessment of foreign protein routing in SMIE cells

In order to determine if SMIE cells are able to route foreign proteins to their predicted locations, we infected cells with several recombinant adenoviruses encoding proteins with distinctive topographical distributions. We chose to transfer the cDNAs using these viruses because we observed that more traditional methods of cDNA transfer (e.g. calcium phosphate precipitation, electroporation) were inefficient; likely because of the cell's small size. As shown in Fig. 5A, when cells were infected with Ad.RSVβgal the encoded protein was found in the nucleus, its expected location. If cells were infected with AdCMVβgal, which lacks a nuclear localization signal, the β-galactosidase was found in the cytoplasm primarily (Fig. 5B). Aquaporin-1, which is not normally produced by SMIE cells [7], was found entirely in the plasma membrane following adenovirus-mediated cDNA transfer (Fig. 5C, D). Finally, ≈92% of the α1-antitrypsin produced by Adα1AT-infected SMIE cells was found in the apical or basal chamber culture media, consistent with its correct sorting as a secretory protein (apical media 3.4 ± 0.2 μg; basal media 5.65 ± 0.22 μg; cell lysate 0.78 ± 0.03 μg; values represent the mean ± SEM of triplicate determinations of the total amount of α1-antitrypsin found in each compartment).

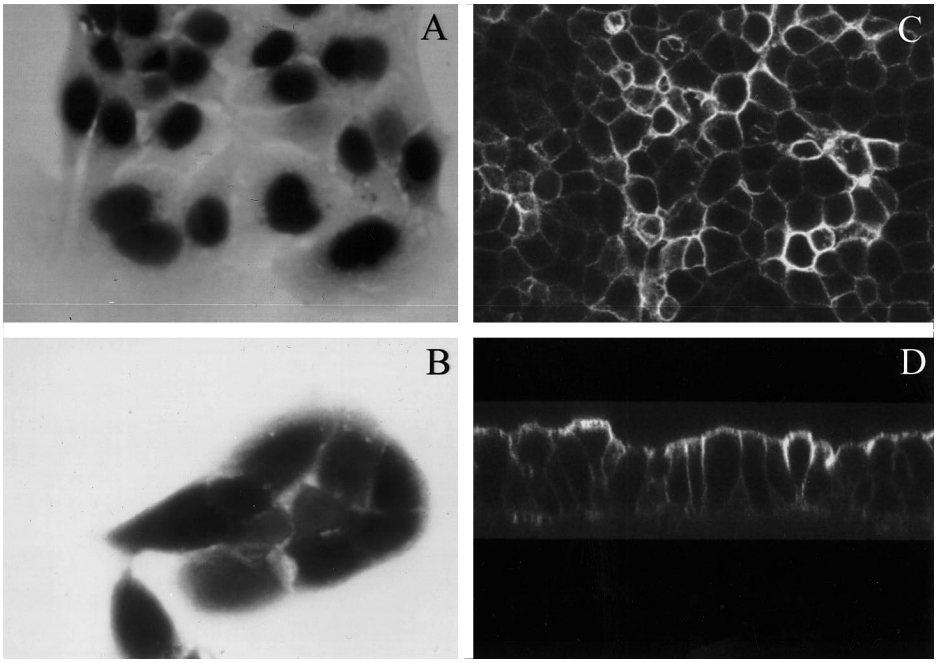

Fig. 5A–D Topographical localization of adenovirus-encoded foreign proteins in SMIE cells. **A** Cells infected with Ad.RSVβgal (a recombinant adenovirus encoding β-galactosidase with a nuclear localization signal); **B** cells infected with AdCMVβgal (a recombinant adenovirus encoding β-galactosidase without a targeting signal); **C, D** confocal images of cells infected with AdhAQP1 (a recombinant adenovirus encoding human aquaporin-1). The image in **C** is of a horizontal (*xy*) optical section, while the image in **D** is of a vertical (*xz*) optical section. Cells in **A** and **B** were stained with X-Gal substrate, and cells in **C** and **D** were immunostained with the affinity-purified antibody to aquaporin-1, as described in Materials and methods

Table 1 Effect of AdhAQP1 infection on net fluid movement across SMIE cell monolayers. SMIE cells were grown on filter inserts as described in the text and infected with either AdhAQP1 (encoding aquaporin-1) or AdCMVhGH (a genetically identical virus but encoding a different transgene, human growth hormone) at a multiplicity of infection ≈5. Transepithelial fluid movement was measured after 60 min as described [7] (*N* = number of experiments)

Virus	*N*	Fluid movement (μl/cm²)
AdhAQP1	3	42.9 ±0.6*
AdCMVhGH	2	7.6 ±1.5

* Significantly different from results (mean ± SEM) with AdCMVhGH-infected cells, $t = 25.7$, $P<0.001$

Assessment of fluid movement across SMIE monolayers

Finally, we assessed the ability of the SMIE cell monolayer to serve as an epithelial barrier across which facilitated fluid movement could be measured. Previously, we have reported that MDCK cell monolayers can be useful for this purpose [6, 7]. As shown in Table 1, when SMIE cell monolayers were infected with AdhAQP1, osmotically directed transepithelial fluid movement was approximately sixfold that seen with cells infected with a control virus, AdCMVhGH. This control virus encodes a transgene product, human growth hormone, which would be unexpected to influence facilitated fluid movement.

Discussion

In this report we have described a rat submandibular gland cell line, SMIE, which when cultured on collagen-coated polycarbonate filters, forms an apparently intact, uniform monolayer which exhibits a polarized morphology, authentic tight junctions and a polarized membrane protein distribution. The general morpholgical appearance of these cells, however, is not that of a well-differentiated salivary cell, but rather seems most consistent with that of a glandular anlage in which a lumen has just formed but further cytodifferentiation has not occurred [21]. Additionally, we showed that SMIE cells are also able to target foreign marker proteins, introduced using recombinant adenoviruses, to their appropriate cellular location. Finally, we have demonstrated that the SMIE cell monolayer is useful for measurement of an important epithelial function: osmotically directed fluid movement. For this purpose we examined fluid movement mediated by a transgene product, human aquaporin-1. Our aggregate findings demonstrate that SMIE cells appear to provide a useful model for the study of some important polarized functions in salivary-gland-derived cells in vitro.

Our interest in commencing these studies was as an initial step to understand the mechanisms by which salivary gland epithelia sort membrane proteins, and achieve a functional polarity. There has been considerable study of the mechanisms responsible for attainment of cell polarity and protein sorting in other epithelia. These studies have been aided by the availability of several model cell lines including MDCK (dog kidney), LLC-PK1 (pig kidney), A6 (from toad bladder), and T84 and Caco-2 (human colonic tumors). These cells, however, may not be entirely appropriate models for questions relevant to salivary glands, as sorting pathways can vary among epithelial subtypes. For example, as pointed out by Dempsey and Coffey [8], MDCK cells generally target newly synthesized membrane proteins directly to either the apical

or basolateral domains while hepatocytes deliver all newly synthesized membrane proteins to the basolateral membrane and shuttle those intended for the apical membrane by a transcytotic process. Furthermore, Caco-2 cells deliver proteins to apical membranes by both direct and indirect pathways. Thus, it seems clear that in order to understand the pathways followed for protein sorting in a particular cell type, it is most useful to study an adequate model of the same cell type [15].

We also have compared SMIE cell behavior in vitro with that of A5 cells, an often studied (e.g. [11, 28]) salivary cell line with immune reactivity to all rat submandibular gland ductal epithelia. A5 cells exhibited disorganized, multilayer growth in vitro on the collagen-coated filters. No distinct basolateral-domain-specific distribution of the α_1-subunit of the Na^+/K^+ATPase was apparent in these cells. Although also not directly presented herein, we studied the growth and behavior of HSG cells, another frequently studied salivary cell line (e.g. [13, 24]), on collagen-coated filters. These cells are derived from a human submandibular gland and reportedly display intercalated-duct-cell-like characteristics. However, HSG cells were unable to form a morphologically intact monolayer on the filters used here for growth. Other available salivary-gland-derived cell lines are much less studied, and to our knowledge there have been no reports, prior to this, of any salivary cell line able to form a polarized monolayer in vitro.

Despite their polarized appearance and the presence of tight junctions, initial examinations of paracellullar permeability showed that cultures of SMIE cells are quite leaky. Measurements of transepithelial electrical resistance were quite low, only ≈30 Ω. cm^2 above the bare filter. Furthermore, the monolayer was also relatively permeable to the water-soluble, membrane-impermeant probes mannitol and dextran (only approx. twofold greater restriction than bare filters alone). Mannitol flux, however, was approximately fourfold greater than dextran flux. Thus, while the SMIE cell monolayer does not form a tight functional barrier, it appears able to discriminate differently sized molecules, and act as a selective molecular barrier. This view is further supported by the studies presented herein of osmotically directed fluid movement across SMIE cell monolayers. In the presence of an expressed transgene encoding aquaporin-1, fluid movement across this in vitro epithelial barrier was markedly greater than that seen in the presence of a control transgene.

In summary, from the results presented in this report we suggest that the SMIE cell line should be a useful experimental tool in helping to understand some polarized functions in a salivary epithelial cell line.

Acknowledgements We are grateful to Dr. Michael J. Caplan for the generous gift of the monoclonal antibody against the α_1-subunit of Na^+/K^+-ATPase. We thank Dr. R. James Turner and Dr. Lawrence A. Tabak for helpful discussions and encouragement, and Ms. Corinne Goldsmith for her technical assistance. We are especially appreciative of the help of Dr. Milton Brightman, NINDS, NIH, in rigorously demonstrating the presence of tight junctions in SMIE cell monolayers.

References

1. Adesanya MR, Redman RS, Baum BJ, O'Connell BC (1996) Immediate inflammatory responses to adenovirus-mediated gene transfer in rat salivary glands. Hum Gene Ther 7: 1085–1093
2. Baum BJ (1993) Principles of saliva secretion. Ann NY Acad Sci 694:17–23
3. Brightman MW, Reese TS (1969)Junctions between intimately apposed cell membranes in the vertebrate brain. J Cell Biol 40: 648–677
4. Cereijido M, Robbins ES, Dolan WJ, Rotunno CA, and Sabatini DD (1978) Polarized monolayers formed by epithelial cells on a permeable and translucent support. J Cell Biol 77: 853–880
5. Cook DI, Young JA (1989) Fluid and electrolyte secretion by salivary glands. In Schultz SG (ed) Handbook of physiology. Section 6: the gastrointestinal system. American Physiological Society, Bethesda, Md., pp 1-23
6. Delporte C, O'Connell BC, He X, Ambudkar IS, Agre P, Baum BJ (1996) Adenovirus-mediated expression of aquaporin-5 in epithelial cells. J Biol Chem 271:22070–22075
7. Delporte C, O'Connell BC, He X, Lancaster HE, O'Connell AC, Agre P, Baum BJ (1997) Increased fluid secretion following adenoviral-mediated transfer of the aquaporin-1 cDNA to irradiated rat salivary glands. Proc Natl Acad Sci USA 94: 3268–3273
8. Dempsey PJ, Coffey RJ (1994) Basolateral targeting and efficient consumption of transforming growth factor-alpha when expressed in Madin-Darby canine kidney cells. J Biol Chem 269:16878–16889
9. Dharmsathaphorn K, McRoberts JA, Mandel KG, Tisdale LD, Masui H (1984) A human colonic tumor cell line that maintains vectorial electrolyte transport. Am J Physiol 246: G204–G208
10. Grasset E, Pinto M, Dussaulx E, Zweibaum E, Desjeux JF (1984) Epithelial properties of human colonic carcinoma cell line Caco-2: electrical parameters. Am J Physiol 247: C260–C267
11. He X, Ship JA, Wu X, Brown AM, Wellner RB (1989) Beta-adrenergic control of cell volume and chloride transport in an established rat submandibular cell line. J Cell Physiol 138 527–535
12. He X, Frank DP, Tabak LA (1990) Establishment and characterization of 12S adenoviral E1A immortalized rat submandibular gland epithelial cells. Biochem Biophys Res Commun 170:336–343
13. He X, Wu X, Turner RJ, Baum BJ (1990) Evidence for two modes of Ca^{2+} entry following muscarinic stimulation of a human salivary epithelial cell line. J Membr Biol 115:159–166
14. He X, Tse C-M, Donowitz M, Alper SL, Gabriel SE, Baum BJ (1997) Polarized distribution of key membrane transport proteins in the rat submandibular gland. Pflügers Arch 433: 260–268
15. Kuliawat R, Lisanti MP, Arvan P (1995) Polarized distribution and delivery of plasma membrane proteins in thyroid follicular epithelial cells. J Biol Chem 270:2478–2482
16. Li J, Nielsen S, Dai Y, Lazowski KW, Christensen EI, Tabak LA, Baum BJ (1994) Examination of rat salivary glands for the presence of the aquaporin CHIP. Pflügers Arch 428:455–460
17. Marrs JA, Napolitano EW, Murphy-Erdosh C, Mays RW, Reichardt LF, Nelson WJ (1993) Distinguishing roles of the membrane-cytoskeleton and cadherin mediated cell-cell adhesion in generating different Na^+, K^+-ATPase distributions in polarized epithelia. J Cell Biol 123:149–164
18. Mastrangeli A, O'Connell B, Aladib W, Fox PC, Baum BJ, Crystal RG (1994) Direct in vivo adenovirus-mediated gene transfer to salivary glands. Am J Physiol 266:G1146–G1155
19. Neufeld TK, Grant ME, Grantham JJ (1991) Measurement of the rate of net fluid secretion by MDCK cells. J Tissue Culture Methods 13:229–234

20. Perkins FM, Handler JS (1981) Transport properties of toad kidney epithelia in culture. Am J Physiol 241:C154–C159
21. Redman RS, Ball WD (1978) Cytodifferentiation of secretory cells in the sublingual gland of the prenatal rat: a histological, histochemical and ultrastructural study. Am J Anat 153:367–390
22. Rodriguez-Boulan E, Powell SK (1992) Polarity of epithelial and neuronal cells. Annu Rev Cell Biol 8:395–427
23. Saier MH Jr, Boerner P, Grenier FC, McRoberts JA, Rindler MJ, Taub M, U HS (1986) Sodium entry pathways in renal epithelial cell lines. Miner Electrolyte Metab 12:42–50
24. Shirasuna K, Sato M, Miyazaki T (1981) A neoplastic epithelial duct cell line established from an irradiated human salivary gland. Cancer 48:745–752
25. Singer KL, Stevenson BR, Woo PL, Firestone GL (1994) Relationship of serine/threonine phosphorylation/dephosphorylation signaling to glucocorticoid regulation of tight junction permeability and ZO-1 distribution in nontransformed mammary epithelial cells. J Biol Chem 269:16108–16115
26. Tse CM, Levine SA, Yun CH, Khurana S, Donowitz M (1994) Na+/H+ exchanger-2 is an O-linked but not an N-linked sialoglycoprotein. Biochemistry 33:12954–12961
27. Turner RJ (1993) Mechanisms of fluid secretion by salivary glands. Ann N Y Acad Sci 694:25–35
28. Yeh CK, Ambudkar IS, Kousvelari E (1992) Differential expression of early response genes, c-*jun*, c-*fos*, and *jun* B, in A5 cells. Am J Physiol G934–G938